European Association for the
Development of Renewable Energies,
Environment and Power Quality (EA4EPQ)

International Conference on Renewable Energies and Power Quality
(ICREPQ'11)
Las Palmas de Gran Canaria (Spain), 13th to 15th April, 2011

Control with floating- and fixed-point DSPs of a low-cost Flexible Platform for a Photovoltaic Grid-Connected System working as an agent in a Distributed Generation Structure

Alexis B. Rey-Boué[1], F. Ruz-Vila[2], José M. Torrelo[3], Salvador Subiela[3]

[1] Dpto. Electrónica, Tecnología de Computadoras y Proyectos
Universidad Politécnica de Cartagena, Edif. Antiguo Cuartel de Antigones (Campus de la Muralla),
Plaza del Hospital, 1, 30202 Cartagena, Murcia (Spain)
Phone:+34 968325928, Fax:+34 968326400, e-mail: alexis.rey@upct.es

[2] Dpto. Ingeniería Eléctrica
Universidad Politécnica de Cartagena, Edif. Hospital de Marina (Campus de la Muralla),
C/Doctor Fleming, s/n. 30202 Cartagena, Murcia (Spain)
Phone:+34 968325351, Fax:+34 968325356, e-mail: paco.ruz@upct.es

[3] Instituto de Tecnología Eléctrica (ITE)
Avenida Juan de la Cierva 24, 46980 Paterna, Valencia (Spain)
Phone:+34 961366670, Fax:+34 961366680, e-mail: jose.torrelo@ite.es, salvador.subiela@ite.es

Abstract. In this paper, a low-cost flexible platform for photovoltaics is developed with a DSP-microcontroller arrangement for doing industrial control in an easy way, and the communication process between them is carried out with the McBSP bus. The control of the DC/DC boost converter and the d-q control approach of the 3-phase Voltage Source Inverter (VSI) have been established: the mathematical model of the plant is described and a decoupled control of the instantaneous active and reactive powers fed to the utility grid is achieved, allowing unitary power factor operation. Several measurements of the involved variables in the platform are described in order to evaluate the performance of the exerted control algorithms with the DSP-microcontroller arrangement, and the development of future complex algorithms and high computational tasks is validated.

Key words

PV Panels, DSP-microcontroller, DC/DC boost converter, 3-phase VSI.

1. Introduction

As an alternative to the traditional pollutant fuel-based Power Generation Plants, the recent liberalization of the electrical market leads to the forthcoming of may dispersed Renewable Generation Systems [1], also known as agents in a Distributed Generation Structure (DG), and capable of feeding energy to the utility grid. These are formed by the Power and Control Subsystems which jointly must guarantee not only the Power Quality [2,3], but also achieve a high efficiency.

Several studies involving the control of different industrial plants with fixed-point Digital Signal Processors (DSPs) are found in the literature [4], where it can be seen its capability of performing 3-phase industrial control algorithms such as Phase Lock Loops (PLLs), Clarke and Park Transformations, PI regulators, Space Vector Modulation (SVM) Techniques, etc., with an appropriate software programming. However, they may lack of additional resources for high-demanding and complex algorithms, such as FIR and IIR filters, Neural Networks Fuzzy Systems and non-linear control, and the use of floating-point DSPs is mandatory [5]. Nevertheless, the floating-point DSPs do not have, in general, on-chip peripherals, and the use of Programmable Logic, such as FPGAs, is needed for doing real-time industrial control [6], yielding new programming paradigms such as Hardware Description Languages (HDL), and new development tools, which increases the development cycles and the overall cost of the project.

To solve the aforementioned situation, this paper proposes a floating- and fixed-point DSP-microcontroller arrangement with the same development tool, and it is structured as follows: firstly, a brief theoretically description of the physical meaning of the variables involved in the connection of Photovoltaic Panels (PV Panels) to the utility grid is carried out, with emphasis in the Power and Control Subsystems, next the Power and the Electronic Control Units with its main modules are explained focussing mainly in the DSP-microcontroller arrangement proposed and, finally, several measurements

are presented to validate the well-function of the low-cost flexible platform.

2. Description of the PV grid-connected system

The PV grid-connected system to be studied is formed by the Power and the Control Subsystems depicted in Fig. 1. The **Power Subsystem** is at the upper side and the **Control Subsystem** is at the lower side.

A. Power Subsystem

The main modules of the Power Subsystem are the **PV Panels**, the **DC/DC boost converter**, the **3-phase VSI**, and the **3-phase utility grid**. It has, among others, the following involved variables: v_P, i_P (voltage and current of the PV panels), i_{IGBT} (current through the IGBT of the DC/DC boost converter), i_D (diode current of the DC/DC boost converter), v_{CC} (dc bus voltage), i_{Clink} (current through the link capacitor C_{link}), i_{CC} (dc bus current), i_u, i_v, i_w (3-phase line currents), i_r, i_s, i_t (3-phase utility grid currents), u_R, u_S, u_T (3-phase utility grid voltage).

The available primary energy of the PV Panels is a function of the incoming irradiance and the variable temperature, through an I-V characteristic curve: the short circuit current is directly proportional to the irradiance, meanwhile the voltage variation can be neglected; on the other hand, the increasing of the temperature reduces the voltage at the PV Panel.

The delivered power can be expressed as follows:

$$p_P = v_P \cdot i_P \tag{1}$$

which is a function of the voltage and current of the PV panels. An algorithm known as maximum power point tracker (MPPT) [7] can be developed to follow the maximum available power of the PV panels.

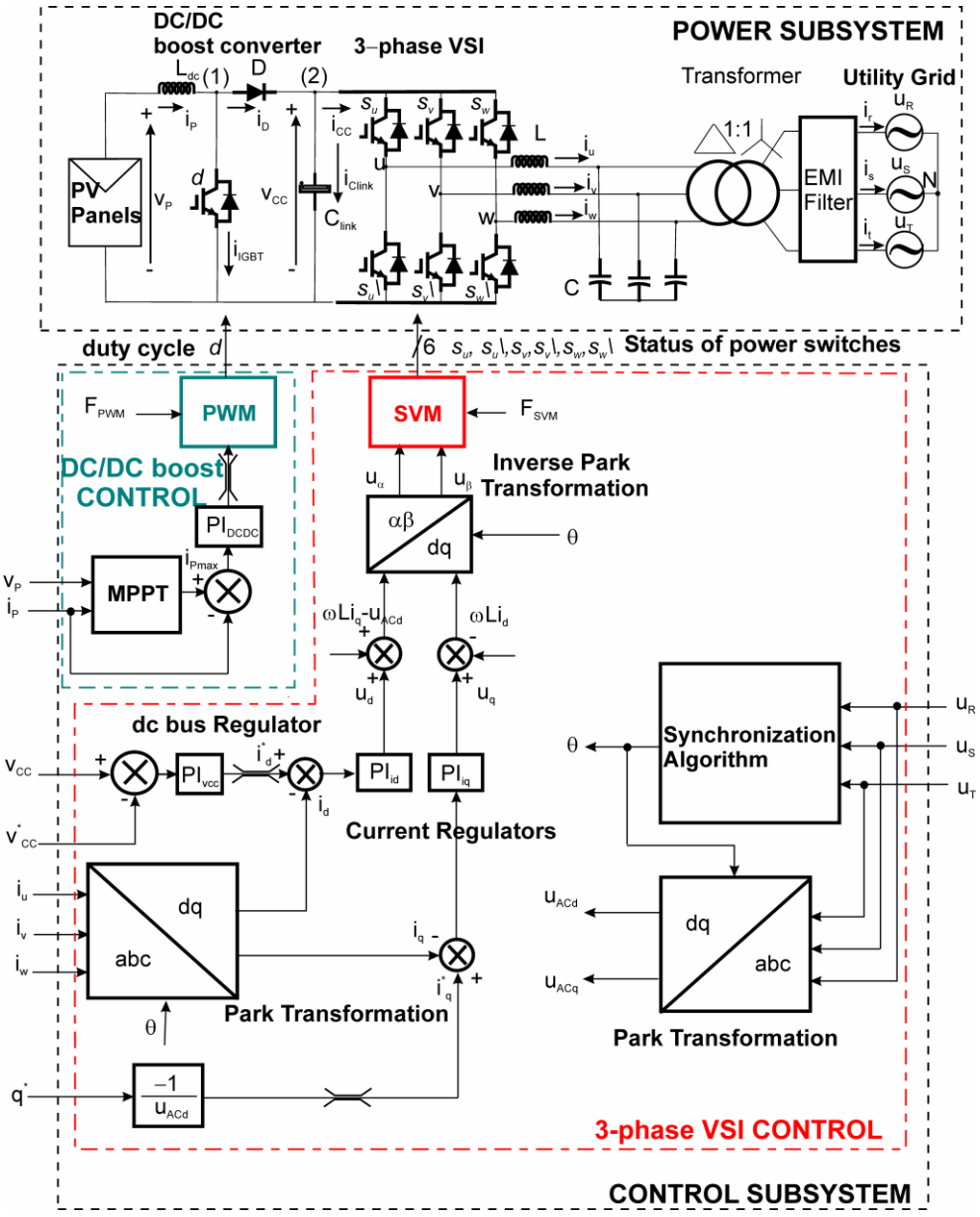

Fig. 1. Block diagram of the 3-phase grid-connected system fed by PV Panels.

In general, the reduced voltage at the output of the PV Panels claims for the use of a DC/DC boost converter, whereas the *dc* nature of the variables involved at the PV Panels needs to be conditioned to the *ac* nature of the 3-phase utility grid voltages by means of the 3-phase VSI (also known as DC/AC converter or inverter) in order to deliver the appropriate instantaneous power into the utility grid with near unitary power factor. The link capacitor C_{link}, the LC filter, the distribution transformer and the EMI Filter are also needed for proper operation and filtering issues.

Neglecting the losses in the distribution transformer, the dynamic of the 3-phase VSI can be described by the following vector equation:

$$\mathbf{u} = R\mathbf{i} + L\frac{d\mathbf{i}}{dt} + \mathbf{u_{AC}} \qquad (2)$$

where **u** is the inverter voltage vector, **i** is the inverter line current vector, $\mathbf{u_{AC}}$ is the utility grid voltage vector, L is the line inductance, and R is the resistance of this inductance. The vector variables are complex and can be calculated as a function of the instantaneous 3-phase inverter voltages u_u, u_v, u_w, the 3-phase line currents i_u, i_v, i_w, and the 3-phase utility grid voltages u_R, u_S, u_T, yielding the space-vector transformation [8]:

$$\mathbf{u,i} = \sqrt{\frac{2}{3}}\left(u_u, i_u + u_v, i_v \cdot e^{j\frac{2\pi}{3}} + u_w, i_w \cdot e^{j\frac{4\pi}{3}}\right),$$

$$\mathbf{u_{AC}} = \sqrt{\frac{2}{3}}\left(u_R + u_S \cdot e^{j\frac{2\pi}{3}} + u_T \cdot e^{j\frac{4\pi}{3}}\right)$$

B. Control Subsystem

The Control Subsystem is fed by several sensed signals coming from the Power Subsystem. Its main modules are the **DC/DC boost Control** module, and the **3-phase VSI Control** module. It has the following additional involved variables: F_{PWM} (DC/DC boost converter's IGBT switching frequency), F_{SVM} (3-phase VSI's IGBTs switching frequency) i_{Pmax} (output reference current of the MPPT algorithm), θ (phase for synchronization purposes), v^*_{CC} (dc bus voltage reference), q^* (instantaneous reactive power reference), *d* (duty cycle for the IGBT of the DC/DC boost converter), s_u, $s_{u\backslash}$, s_v, $s_{v\backslash}$, s_w, $s_{w\backslash}$ (status of the IGBTs of the 3-phase VSI), u_d, u_q, i_d, i_q, u_{ACd}, u_{ACq} (*d-q* synchronous reference frame components of **u**, **i**, and $\mathbf{u_{AC}}$ vectors, respectively), u_α, u_β (α-β stationary reference frame components of vector **u**).

According to the input dc voltage and current in the PV Panels (v_P, i_P) and the output dc bus voltage (v_{CC}), the MPPT algorithm gives, for a specific irradiance and temperature, the optimal command reference current (i_{Pmax}) to the current regulator PI_{DCDC} that feeds the PWM sub-module in order to compute the proper duty cycle *d* for the DC/DC boost converter.

The 3-phase VSI Control module is made by the **Synchronization algorithm**, the two cascaded loops made by the fast inner **current regulators** and the slow outer **dc bus voltage regulator**, as well as the SVM sub-module [9], which computes the adequate status of the 3-phase power switches in the 3-phase VSI for closing the loop with the desired behaviour.

The Synchronization algorithm [10] is the responsible of attaining the proper synchronization in phase and frequency of the 3-phase inverter line currents and the utility grid voltages, so as to achieve a unitary power factor in the connection if wished.

The inner current regulators are the responsible of the power quality and protections; the implementation of a **d-q control** approach [11] allows the decoupled control of the instantaneous active power *p* and the instantaneous reactive power *q* if $\mathbf{u_{AC}}$ is aligned with the **d** axis in the rotating synchronous reference frame (u_{ACq}=0). For this:

$$\begin{aligned} p &= u_{ACd}\, i_d \\ q &= -u_{ACd}\, i_q \end{aligned} \qquad (3)$$

The outer dc voltage regulator holds the dc bus v_{CC} at the desired command reference (v^*_{CC}), allowing the maximum power transfer from the PV Panels into the utility grid by delivering the proper command reference of the *d* component of **i** (i^*_d) to the inner current regulator PI_{id}. If the looses in the DC/DC boost converter and in the 3-phase VSI are neglected, $p=p_P$ and i^*_d will be proportional to the available power in the Solar Panels. On the contrary, the quadrature command reference of **i** (i^*_q) is the responsible of controlling the power factor of the inverter-grid connection with the other inner current regulator PI_{iq}. So, equating (1) and (3), yields:

$$i^*_d = \frac{p_P}{u_{ACd}} = \frac{v_P i_P}{u_{ACd}}, \quad i^*_q = \frac{-q^*}{u_{ACd}} \qquad (4)$$

3. Power and Electronic Control Units

The **Power Unit** is basically implemented with IGBTs, meanwhile the **Electronic Control Unit** (see its block diagram in Fig. 2) is basically implemented with two evaluation module boards[1]: the floating-point TMS320C6713 DSP Starter Kit and the eZdsp™F2812 Starter Kit based on the 32 bits fixed-point TMS320F2812 microcontroller for exerting digital control (the ***DSP-microcontroller arrangement***), both chips from *Texas Instruments*[2]; the former is responsible of executing complex and high-demanding algorithms due to its floating-point *core* and the 16Mbytes of synchronous DRAM memory, whereas the latter is used mainly in control tasks and for firing the power switches

[1] [Online]:http://www.spectrumdigital.com/
[2] [Online]: http://www.ti.com/

of the IGBTs due to the large amount of integrated on-chip peripherals. Both controllers have on-chip non-volatile Flash memories that allow, in addition to the emulation-based operation for debugging tasks, a complete standalone operation valid for the development of low-cost prototypes.

Several 10th order low-pass FIR filters are developed in the floating-point DSP to be imposed to the measured and conditioned 3-phase utility grid voltages and line currents through its MsASP bus. These filters are design with cutoff frequencies f_c=500Hz and a very small delay for the sensed voltages, avoiding the degradation of the power factor, and reducing the high order harmonic distortions produced by the commutations of the power switches.

In addition, the block diagram of Fig. 2 also shows an expansion block for the 3-phase grid currents in order to compensate the low-frequency harmonic distortion produced by the presence of nonlinear loads.

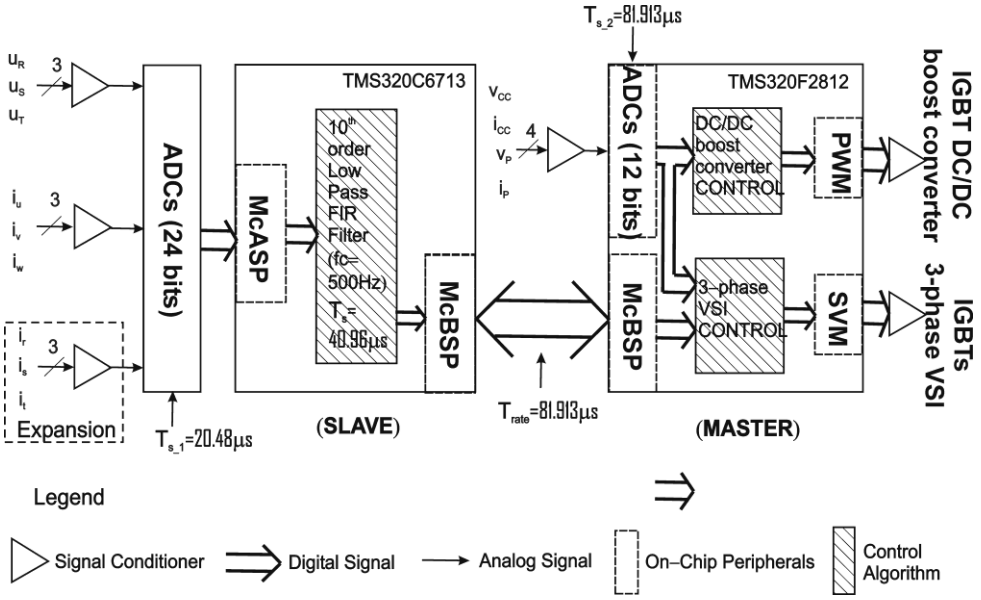

Fig. 2. Block diagram of the Electronic Control Unit.

The output filtered signals at the TMS320C6713 DSP are sent to the TMS320F2812 microcontroller (working as the Master in the communication process) via the McBSP communication bus, which supports the Time Division Multiplexed (TDM) protocol, at a rate of 81.913µs.

For this work, 16 channels are used for the communication of data from TMS320C6713 towards the TMS320F2812 and other 16 channels for the communication in the opposite direction.

The dc input variables (v_{CC}, i_{CC}, v_P, i_P) are measured, conditioned and fed to the on-chip-peripheral 12-bit ADC module, sample at a rate of 81.913µs in the TMS320F2812 microcontroller itself, which is the responsible of executing the following algorithms in real-time:

- MPPT algorithm and DC/DC boost converter Regulation
- dc bus Regulation
- 3-phase VSI-utility grid Synchronization
- Current Regulation
- PWM algorithm with on-chip peripheral
- SVM algorithm with on-chip peripheral

Finally, one optocoupled signal is sent to fire the IGBT of the DC/DC boost converter and 6 optocoupled signals are sent to the power module for firing the IGBTs of the 3-phase VSI.

It must be said that the functionality of the flexible platform is achieved through an intelligent use of the interrupt capabilities of both, the DSP and the microcontroller. **XINT1()** is the hardware interrupt for the Zero-cross detector, **XINT2()** configures a push-button as a hardware interrupt in order to control the Emergency Seta so as to stop the delivering of energy to the utility grid if needed, **MXINTA()** and **MRINTA()** are the responsible of sending and receiving information from the TMS320C6713 by the McBSP bus, and the activation of a flag when the communication process is periodically established, and **TIMER4()** controls that the system is running periodically according to the pre-established parameters, tests the frequency of the utility grid voltage, and deals with the anti-islanding phenomena when the utility grid goes out.

Code Composer Studio v.3.1 is the development tool for debugging, compiling and flash programming tasks.

4. Experimental results

The experiment setup is depicted in Fig. 3, where a photograph of the built flexible platform is shown, and the

electronic modules of the Power and Control Units are highlighted in red.

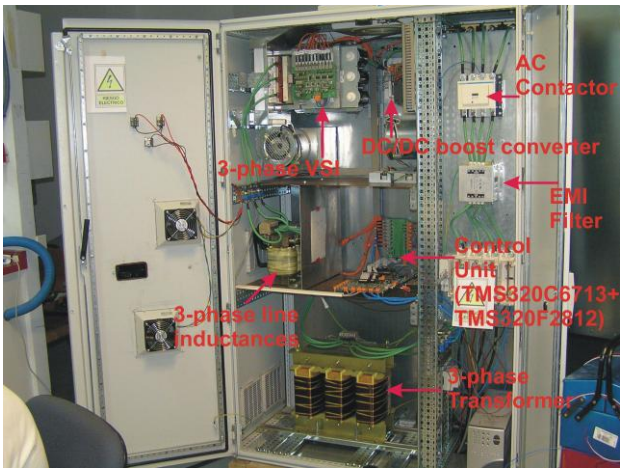

Fig. 3. The low-cost flexible platform.

Following, a simulated 10kW PV Panel is configured to deliver energy into the 3-phase utility grid. For this, the Power Unit is made with the DC/DC boost converter and the 3-phase VSI, and several experiments have been set up for doing the measurements of the industrial variables that validate the proper performance of the flexible platform.

The DC/DC boost converter includes the 1.5mH-2200µF LC section and the *SKiiP 642 GB120-2DL* IGBT electronic kit, meanwhile the 3-phase VSI is built with the 6-pack-integrated intelligent Power System *SkiiP 513GD172-3DUL*, which includes the IGBTs semiconductors for the 3-phase power switches, both from *Semikron* and configured to work at 12.208KHz of PWM switching frequency. The latter includes the 1.1mH-4µF Y-connected LC filter for reducing the ripple in the line currents due to the switching-based operation of the IGBTs semiconductors.

The distribution transformer for the inverter-grid connection is also used due to the normatives on security issues, which has a Y-connected in the primary side (grid side), and a Δ-connected in the secondary side (inverter side). Neglecting the magnetizing effect, its equivalent output inductance is 640µH.

The Electronic Control Unit is mainly made by the DSP-microcontroller arrangement as said before, and the electronic circuitry for the signal conditioning purposes.

A. Tests for the DC/DC boost converter

Firstly, the **DC/DC boost converter**, with a resistive load of two 156Ω parallel resistors, is tested. The input and output nominal voltages are 250V and 600V, respectively, and a nominal duty cycle of 0.583 is achieved. The DELTA SM300-20 dc power source is used for feeding the input voltage, whereas the AVTRON LPH-60 resistive load bank is used to simulate load steps. The design input and output constraints are that a minimum input voltage of 33% of the nominal voltage is required to guarantee the rated output nominal voltage, meanwhile a variation of 5% is allowed over the nominal output voltage.

1) dc output response to load step

Fig. 4 shows the time evolution of the output voltage (red-color), the input voltage (green-color), and the flowing current through the parallel load resistor (blue-color). Again, the output voltage remains inside the ±5% fluctuation band when a 50% load step is applied by connecting a parallel resistor of the same value.

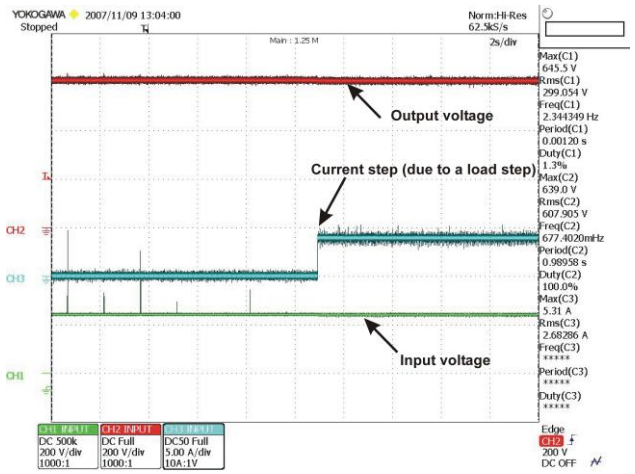

Fig. 4. dc output response to load step.

B. Tests for the 3-phase VSI

Secondly, the **3-phase VSI** is tested. PV panels are simulated by the AMREL HPS800-180-D013 programmable dc power source in order to deliver 10kW of active power. The input constrain is 600V in the dc bus, whereas the output constrains are 230V rms for the nominal voltage and 50Hz for the fundamental frequency of the 3-phase utility grid. The LCL branch is built with the 1.1mH-4µF LC filter (mentioned above) and the inductance of the distribution transformer (640µH). The Fluke 430 Series Three-Phase Power Quality Analyzer is used for power quality measurements.

1) Unitary power factor connection

Fig. 5 displays the time evolution of the utility grid voltage and current at phase 1 with unitary power factor connection. The rms values of the utility grid voltage and current are 230.6V and 12.4A, respectively, and the synchronization in phase and frequency is achieved. The Power and Energy Table depicted at the right-half part of the figure shows a total apparent power of 9 kVA, and a total active power of 8.92 kW, with 0.99 power factor of the inverter-grid connection.

In spite of the absence of harmonic distortions in the utility grid voltage, the harmonic distortion of the grid current is due to the non-linear behavior of the employed distribution

transformer, though it is below the limits imposed by IEC 61000-3-2 normative [3]. Then, the adequate Power Quality of the inverter grid-connection is assured.

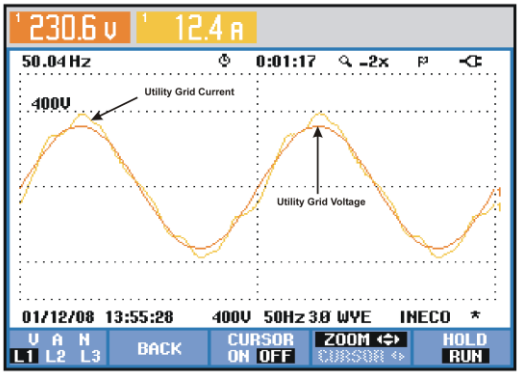

(a)

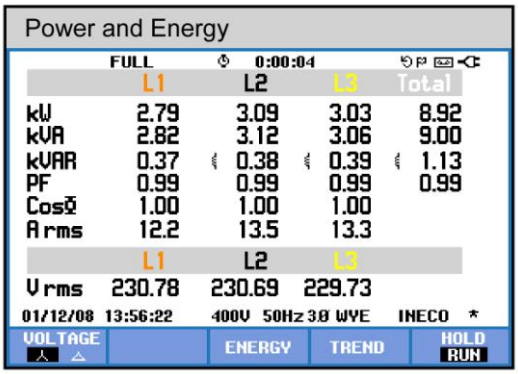

(b)

Fig. 5. a) Time evolution of the utility grid voltage and current at phase 1 for unitary power factor connection.
b) Power and Energy Table.

5. Conclusion

This paper presents a floating- and fixed-point DSP-microcontroller arrangement in order to control a flexible platform for Photovoltaic grid-connected systems. The floating-point *core* of the DSP allows the development of control algorithms in a natural way, running faster and in a compact-manner, and its available high capacity of DRAM and on-chip Flash memories allows the development of complex algorithms and high computational tasks. On the other hand, the wide on-chip peripherals resources of the microcontroller, such as timers, PWM generation, communication buses, etc., can be used for specific and pre-programmed tasks, together with classic industrial control algorithms.

Though several discrete FIR filters for 3-phase utility grid and line currents are developed in the TMS320C6713 floating-point DSP, any kind of future complex algorithm can be used with minimal changes if time constrains in the communication protocol are observed.

The experimental results show the validity of the proposed DSP-microcontroller arrangement for doing real-time control of the flexible platform for Photovoltaic grid-connected systems according input and output constrains.

Finally, Starter Kits of the DSP-microcontroller arrangement, including software tools, are available at a low-cost, and can be used for both, the development of prototypes and also for final products.

Acknowledgement

This work has been supported by a grant from the Spanish Government as a part of project ENE2005-09375-C03-01/CON, entitled “Gestión de la microproducción conectada a redes eléctricas con alta penetración de generación distribuida”.

References

[1] F. Blaabjerg, Z. Chen, and S. Baekhoej-Kjaer, "Power Electronics as Efficient Interface in Dispersed Power Generation Systems", in IEEE Transactions on Power Electronics 2004, Vol. 19(5), pp. 1184-1194.

[2] Recommended Practices and Requirements of Harmonic Control in Electrical Power Systems. Standard ANSI/IEEE 519-1992.

[3] Limits for harmonic current emissions (equipment input current <= 16 A per phase). IEC Std. 61000-3-2. International Electrotechnical Commission, IEC 1995.

[4] R. Gopinath, S. Kim, J-H. Hahn, P.N. Enjeti, M.B. Yeary, and and J.W. Howze, "Development of a Low Cost Fuel Cell Inverter System With DSP Control", in IEEE Transactions on Power Electronics 2004, Vol. 19(5), pp. 1256-1262.

[5] R. Alcaraz, E.J. Bueno, S. Cobreces, F.J. Rodríguez, F.Huerta, and M. Liserre, "Comparison of Voltage Harmonic Identification Algorithms for Three-Phase Systems", in IECON 2006, pp. 5179-5184.

[6] F.J. Rodríguez, S. Cobreces, E.J. Bueno, Á. Hernández, R. Mateos, and F. Espinosa, "Control electronic platform based on floating-point DSP and FPGA for a NPC multilevel back-to-back converter", in ELSEVIER Electric Power Systems Research 2008, Vol. 78, pp. 1597-1609.

[7] T. Tafticht, K. Agbossou, M.L. Doumbia, and A. Cheriti, "An improved maximum power point tracking method for photovoltaic systems", in ELSEVIER Renewable Energy 2008, Vol. 33, pp. 1508-1516.

[8] J. M. Aller, A. Bueno, and T. Pagá, "Power System Analysis Using Space-Vector Transformation", in IEEE Transactions on Power Systems 2002, Vol. 17(4), pp. 957-965.

[9] M.P. Kazmierkowski, M.A. Dzieniakowski, and W. Sulkowski, "Novel Space Vector Based Current Controllers for PWM-Inverters", in IEEE Transactions on Power Electronics 1991, Vol. 6(1), pp. 158-166.

[10] A. Timbus, R. Teodorescu, F. Blaabjerg, and M. Liserre, "Synchronization Methods for Three Phase Distributed Power Generation Systems. An Overview and Evaluation", in PESC 2005, pp. 2474-2481.

[11] M. Chinchilla, S. Arnalte, J.C. Burgos, and J.L. Rodríguez, "Power Limits of grid-connected modern wind energy systems", in ELSEVIER Renewable Energy 2005, Vol. 31, pp. 1455-1470.